Available online at www.sciencedirect.com
ScienceDirect
Trans. Nonferrous Met. Soc. China 24(2014) 1393−1399
Transactions of Nonferrous Metals Society of China
www.tnmsc.cn

Microstructure and mechanical properties of GTA weldments of titanium matrix composites prepared with or without current pulsing

Jian-wei MAO, Wei-jie LÜ, Li-qiang WANG, Di ZHANG, Ji-ning QIN

State Key Laboratory of Metal Matrix Composites, Shanghai Jiao Tong University, Shanghai 200240, China

Received 22 May 2013; accepted 14 January 2014

Abstract: The effects of current pulsing on the microstructure, hardness and tensile properties at different temperatures of gas tungsten arc (GTA) weldments of titanium matrix composites were studied. Full-penetration butt joints were made with or without current pulsing. Optical microscopy, hardness test and scanning electron microscopy were employed to evaluate the metallurgical characteristics of welded joints. Tensile properties of weldments at different temperatures were studied and correlated with the microstructure. The results exhibit that current pulsing leads to the refinement of the weld microstructure and TiB whisker and the redistribution of reinforcements resulting in higher hardness, tensile strength and ductility of weldments in the as-welded condition.
Key words: titanium matrix composites; pulsed current; welding; mechanical properties; grain refinement; microstructure

1 Introduction

In situ discontinuously reinforced titanium matrix composites (TMCs) have attracted much attention in academic research and industry applications because they offer a combination of good mechanical properties [1], superior creep resistances [2], high strength and metallurgical stability at room and high temperatures [3], which make them candidate materials for aerospace, nuclear, energy and automotive applications, etc [4]. However, the development of new manufacturing techniques plays a significant role in exploiting TMCs in new fields of applications. Recently, the interest in welding of TMCs has been increased rapidly, mainly concentrating on argon-arc welding, laser beam welding and friction welding [5−7].

Gas tungsten arc welding (GTAW) is the most widely used process for joining titanium and titanium alloys, especially for thin sheets owing to its easier applicability, flexibility and better economy [8,9]. The drive to improve the weld quality interrelated to the improvement in process parameters demands the use of improved welding techniques and materials. Welding of titanium leads to grain coarsening in the fusion zone and heat affected zone. In conventional welding, weld fusion zones usually show coarse columnar grains, because of the prevailing thermal conditions during weld metal solidification [10]. This generally results in inferior weld mechanical property and poor resistance to hot cracking.

Pulsed current gas tungsten arc welding (PCGTAW) is a variation of GTAW which involves cycling the welding current at a given regular frequency. In current pulsing method, the peak current is selected to produce adequate penetration and bead contour, while the background current is set at a level enough to maintain a stable arc [11]. This permits arc energy to be used effectively to fuse a spot of controlled dimension in a short time producing the weld as a series of overlapping nuggets. Current pulsing enhances fluid flow, reduces temperature gradient, increases cooling rate and causes a continual change in the molten puddle size and shape leading to the microstructure refinement, and this in turn results in enhanced mechanical performance of the joint by changing weld pool solidification conditions [12]. Metallurgical advantages of PCGTAW include reduced width of heat affected zone, refinement of fusion zone grain size and substructure, control of segregation, etc [13]. Current pulsing has been applied to obtaining grain refinement in weld fusion zones and improvement in

Foundation item: Project (51371114) supported by the National Natural Science Foundation of China; Project (2012CB619600) supported by the National Basic Research Program of China; Project (10SG15) supported by the Dawn Program of Shanghai Education Commission, China; Project (12XD1402800) supported by Shanghai Science and Technology Committee, China
Corresponding author: Wei-jie LÜ; Tel: +86-21-34202641; Fax: +86-21-34202749; E-mail: luweijie@sjtu.edu.cn
DOI: 10.1016/S1003-6326(14)63204-0

weld mechanical properties of Ti alloys [9−13]. However, there are no data available relating current pulsing and mechanical properties of TMCs joints. Therefore, an attempt has been made to study the effect of current pulsing on mechanical behaviors of TMCs joints by PCGTAW.

2 Experimental

2 mm rolled sheets of TMCs in the annealed condition were used as the base materials. The reinforcements used were TiB whisker (TiB_w) and La_2O_3 particle with the additions of 1.26% and 0.58% (volume fraction) respectively. Chemical compositions (mass fraction, %) of the base material were 6.0 Al, 3.6 Sn, 4.1 Zr, 1.0 Nb, 0.2 Mo, 0.34 Si and balance Ti. Coupons with dimensions of 130 mm×55 mm×2.0 mm sliced from the sheet were mechanically wire brushed, acid pickled in a $HF+HNO_3$ mixed solution and cleaned with acetone prior to welding. Square butt joint (Fig. 1(a)) was used to make the welds. Single pass, autogenous welding procedure (without filler metal addition), was performed to fabricate the joints perpendicular to the rolling direction of sheets with or without current pulsing. Due to the high affinity of titanium to atmospheric gases at high temperatures, high purity (99.99%) argon gas was used as shielding gas in the welding process. The welding parameters used are listed in Table 1.

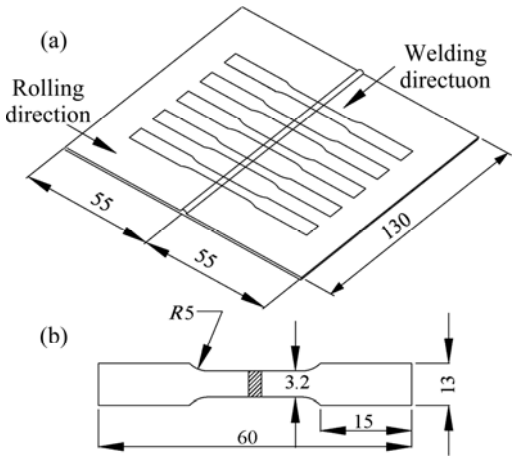

Fig. 1 Dimensions of joint configuration (a) and tensile specimens (b) (unit: mm)

After preparation of joints, the welded joint was sliced and then machined to the required dimensions (Fig. 1(b)) for preparing tensile specimens. Tensile tests were performed at a constant strain rate of 1.2×10^{-3} s^{-1} for the base metal and joints at different temperatures (298, 873 and 923 K). Three different samples were made to evaluate the longitudinal tensile properties.

For optical microstructural studies, the joints were transverse sectioned at the vertical axis of welding direction by a linear cutting machine. Cross-sectional samples were grinded with different grades of water abrasive papers, polished with Cr_2O_3 water solution and finally etched with a 2% HF + 8% HNO_3 (volume fraction) solution to reveal the microstructure. Microstructural analysis was conducted by an optical microscope (Make: ZEISS, Germany; Model: Axio Imager A1m) incorporated with an image analyzing software (Metal Vision) and scanning electron microscope (Make: FEI, America; Model: Quanta FEG 250). Vickers hardness tests were executed at intervals of 0.2 mm across the joint by a diamond pyramid indenter under a load of 1.96 N for 30 s.

Table 1 Welding parameters

Welding process	Parameter	Value
Unpulsed welding	Arc current/A	120
	Arc voltage/V	12
	Travel speed/(cm·min^{-1})	30
Pulsed welding	Peak level (I_p)/A	125
	Background level (I_b)/A	50
	Pulse frequency/Hz	4
	Travel speed/(cm·min^{-1})	30
	Pulse-on time	50%
	Arc voltage/V	14
	Shielding gas	Argon, 99.99%
	Shield gas flow rate/(L·min^{-1})	14
	Electrode	Cerium−tungsten, 2 mm diameter

3 Results and discussion

3.1 Weld bead geometry

The molten pool profile, cooling speed and grain growth rate are all associated with the welding heat input in the base metal during welding. The heat input rate in the welding and the cooling rate after welding deeply affect the grain size and phase formation. It is necessary to study the effect of heat input on the bead shape. Typical weld bead profile is shown in Fig. 2(a) and macrographs in unpulsed and pulsed condition are shown in Fig. 2(b). The weld bead geometries are measured by a stereomicroscope. The weld bead profiles and related dimensions are seen in Table 2.

In both unpulsed and pulsed conditions, there is no evidence of welding defects in the joints. It can be seen from Fig. 2(b) and Table 2, in the constant current process, weld width and back height are obviously higher than those by pulsed current process, which is attributed to higher heat input of GTAW [9]. Comparatively, an appreciable variation in the width and reinforcement of

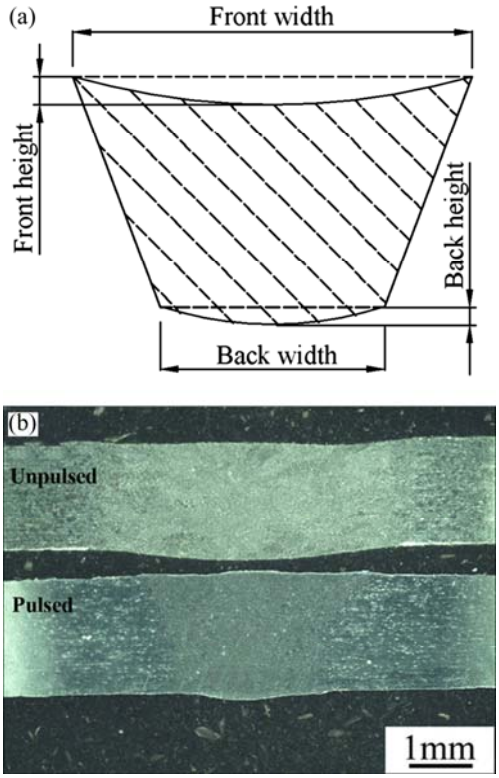

Fig. 2 Typical weld bead profile (a) and macrograph of joints (b)

Table 2 Weld bead parameters of TMCs

Weld bead parameter	Unpulsed	Pulsed
Front width w_f/μm	298.49	219.77
Back width w_b/μm	260.34	97.57
Front height/μm	2.90	1.93
Back height/μm	11.59	6.52
Depth of penetration (H)/μm	1.95	1.92
φ (w_f/H)	153	114.00
R_w (w_f/ w_b)	0.87	0.44

weld is evident from the macrostructure of the pulsed joints due to the varied heat input to the weld, and the macrostructure of pulsed joints shows a trapezoidal shaped weld region (Fig. 2(b)). The aspect ratio of weld (φ) and back width to front width ratio (R_w) in PCGTAW are lower than those by the constant current process. The R_w variation reflects the full penetration stability of the PCGTAW process of TMCs. This proves that the welded joint made by PCGTAW has a better appearance than that by GTAW.

3.2 Microstructure characteristics of welded joints

As analyzed in our earlier researches [5], the weld has four distinct microstructure zones, named as fusion zone (FZ), bond area (BA) and heat affected zone (HAZ) as well as base metal (BM). Figure 3 displays the SEM images of different weld regions in the PCGTAW joint compared with those of the GTAW joint.

As shown in Fig. 3(a), the base metal is composed of α and β phases at grain boundaries. TiB whisker reinforcements are dispersed in the matrix and La_2O_3 particles are not found due to their nanoscale size [3]. The weld microstructures are essentially different from those of the BM at both two conditions. The FZ presents typical columnar grains (Figs. 3(b) and (e)) and the BA exhibits coarse equiaxed grains (Figs. 3(c) and (f)). Moreover, a perceptible difference in grain sizes is found in FZ and BA at two conditions. This fact reveals that the current pulsing plays a very active role in the weld microstructure. The columnar grain size of FZ in pulsed condition is smaller than that in unpulsed condition and the mean grain size of 40 μm for BA in the former is lower than 60 μm in the latter. Besides, some white substances are redistributed at β columnar grain boundaries in the weld, forming a network structure due to the grain refinement in both two conditions, and the enlarged images reveal that they are TiB_w reinforcements (Figs. 4(a) and (b)) and confirmed by the EDS analysis

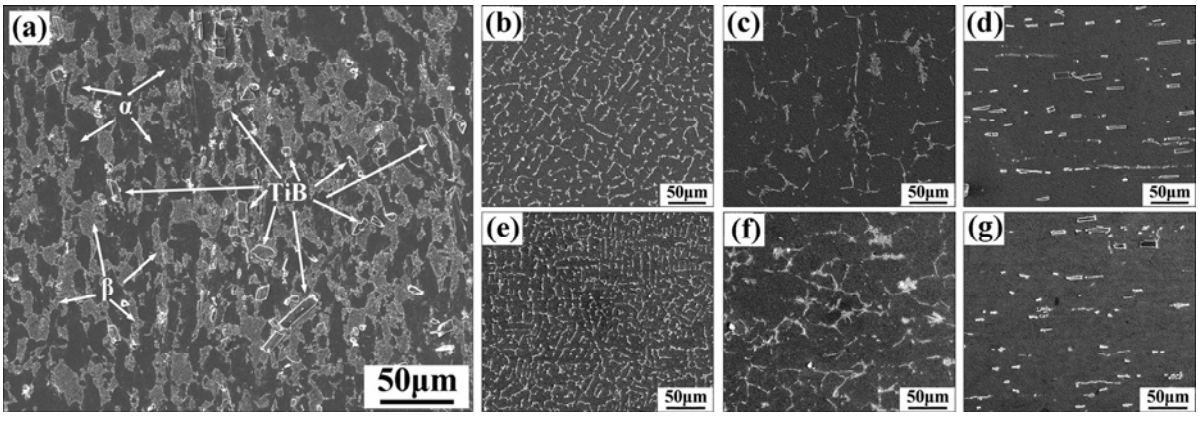

Fig. 3 SEM images of BM (a) and weld regions of FZ (b), BA (c), HAZ (d) for unpulsed weld, FZ (e), BA (f), HAZ (g) for pulsed weld

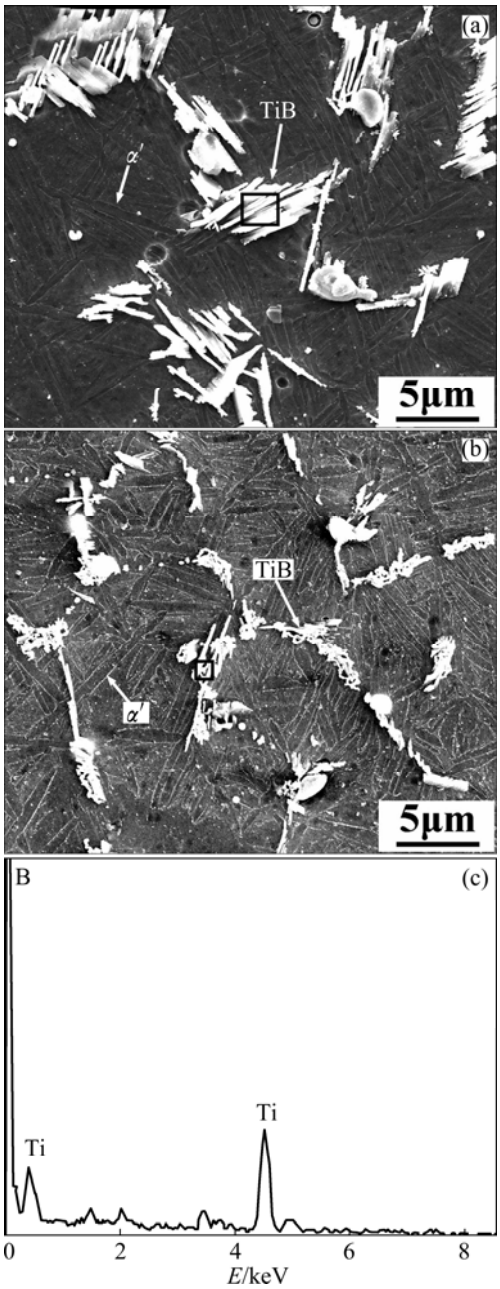

Fig. 4 Enlarged SEM images of FZ in unpulsed (a) and pulsed (b) conditions, and EDS analysis (c) of square in Fig. 4(a)

(Fig. 4(c)). This is attributed to the remelting and reforming of TiB during the welding process [5]. Besides, in pulsed condition the extent of TiB_w clustering at grain boundaries (Fig. 4(b)) visibly decreases compared with that in unpulsed condition (Fig. 4(a)) because of the effect of current pulsing. Although the microstructure in HAZ is similar with that in BM in two conditions, TiB_w in HAZ shows a bit smaller size and more uniform distribution than that in BM, and the amount of TiB in HAZ at unpulsed condition is a bit higher than that at pulsed condition, which is ascribed to the greater weld heat input in the former. A comparison of the pulsed and unpulsed welds reveals that pulsing results in grain refinement and smaller sizes and more uniform distribution of TiB_w in the weld although the degree of grain refinement is not considerable.

Pulsing is also found to have great effects on the β phase transformation in FZ (Fig. 4). From Fig. 4, it can be known that the β columnar grains are composed of α' martensites, forming a typical basket-weave structure because the welded joints were heated over β-transus temperature [14] and rapidly air cooled, so the diffusionless transformation ($\beta \rightarrow \alpha'$) will take place [10,11]. Moreover, the α' laths in fusion zone exhibit a slightly lower aspect ratio in the pulsed weld compared with the unpulsed weld. In unpulsed condition, the α' laths are a little bigger with length and width of 5.55 and 0.742 μm, respectively, while the α' laths are short and thin with length and width of 4.52 and 0.581 μm separately in the pulsed condition. This phenomenon is also found by BABU et al [12], which is due to the changes of welding heat input.

In PCGTAW technique, pulsed current welding is obtained by pulsing the current between the peak current and background current. The pulsing of the welding current has influence on the solidifying weld pool by affecting the weld temperature distribution, causing increased fluid motion and lowering the thermal gradients in the front of solid/liquid interface [11]. SUNDARESAN et al [15] proved that the grain refinement is ascribed to the effect of pulsing on thermal gradients, fluid flow and weld pool shape. Due to the temperature fluctuations inherent in pulsed welding, the continual changes in the weld pool shape and the periodic interruptions during the grain growth process happen. Thus, the direction of the maximum temperature gradient at weld pool boundary also changes continuously with time. As a result, new grains successively become favorably oriented with respect to the instantaneous direction of the maximum thermal gradient. Therefore, each grain grows only a small distance and more grains grow leading to fine-grained structure. The grain refinement observed in pulsed welding has been ascribed to a mechanism involving dendrite fragmentation [9]. Owing to the effect of pulsed current, the cyclic temperature changes at the solid/liquid front cause remelting and breaking-off of the growing dendrites and these fragments become sites for heterogeneous growth which finally hinder the columnar growth process. Moreover, the pulsed current positively causes great supercooling of the liquid metal in the weld pool due to suddenly reducing the heat input to the weld pool under the background current condition [16], which enhances the cooling rate, and this will promote numerous nucleations in weld pool which eventually leads to fine grains [17]. When pulsed current is applied, the agitaion of pulsing and rapid cooling of weld pool

will cause the refinement and more uniform of TiB_w in the weld. Pulsing has promoted the decomposition of the β phases by diffusionless reaction [13], which reveals that pulsing increases the cooling rate during the welding. Therefore, such a change in cooling rate will result in much finer size of α' martensite due to the higher cooling rate.

3.3 Microhardness test

Hardness profiles were measured along the mid-thickness line of the butt-joints cross-section and the results are shown in Fig. 5. The hardness of BM is $HV_{0.2}$ 444 and the standard error (SE) is 0.911.

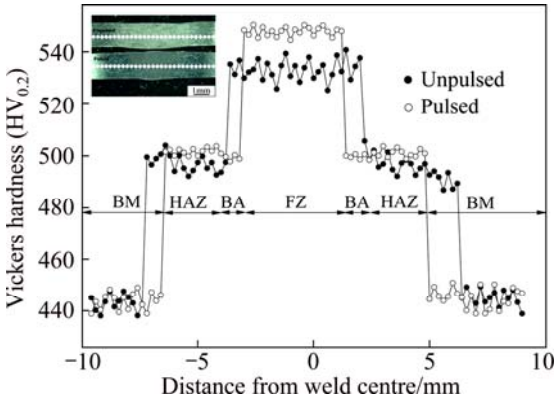

Fig. 5 Hardness profiles across welds in two conditions

In both two conditions, the weld exhibits higher hardness than the base metal, and the harness reaches the maximum in FZ. This is ascribed to the presence of α' martensite and the network structure of smaller TiB_w in the weld. BABU et al [12] proved the strengthening effect in the weld followed by the microstructural transformation from the intergranular β into α' due to the rapid cooling of the molten pool. It is worth noting that the hardness of weld seam increases by 24% in pulsed condition and 20% in unpulsed condition. Besides, the fluctuation extent of hardness in pulsed condition is far lower than that in unpulsed condition and the SE of 0.366 of hardness measurement in pulsed condition is quite less than 0.747 in unpulsed condition, which reveals that the pulse welding microstructure is more uniform and refined compared with that in unpulsed condition. The fusion zone made by pulsing shows a higher hardness (548 $HV_{0.2}$), increased by 3% compared with unpulsed welds (533 $HV_{0.2}$). This phenomenon of hardness increase in the pulsed weld was also observed by other researchers [18, 19], and they believed that the increase in hardness can be ascribed to the microstructural transformation and the refinement of microstructure and reinforcement in the weld.

In the BA and HAZ, although the average hardness in pulsed condition is gently higher than that in unpulsed condition due to the more fined and uniform microstructures, it is almost the same in the welding condition. The harness values in unpulsed condition of the HAZ and BA are $HV_{0.2}$ 496 and $HV_{0.2}$ 499 respectively, and the corresponding hardness values in pulsed condition are $HV_{0.2}$ 499 and $HV_{0.2}$ 501, which are higher than that of the BM, increased by 11.7%, 12.4% and 12.8% in turn. Moreover, the hardness in BA seems to decrease slightly compared with HAZ, which is also observed in literature [7]. This fact reveals that the pulsing used has a trifling effect on the BA and HAZ, and in both two welding conditions the adverse effect due to the coarse grains is much greater than the strengthening effect of finer TiB, which results in similar average hardness in BA and HAZ.

3.4 Tensile properties

Based on the early research results, the mechanical properties of welded joint are positively related to the weld microstructure. One of the objectives of this study is to see whether the observed grain refinement led to an improvement in the tensile properties of PCGTAW joints. To this end, the unpulsed welds were compared with the pulsed welds. The tensile properties of base metal were also included for comparison. Figure 6 shows the variation of the ultimate tensile strength (UTS) and elongation with temperature for the weldments and base metal.

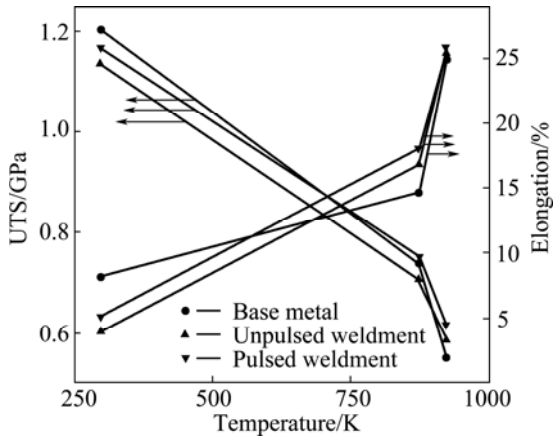

Fig. 6 Variation of UTS and elongation with temperature for base metal and weldments

At 298 K, the UTS of the base metal is 1202 MPa, and the strength of unpulsed joints is 1135 MPa, 5% slight reduction in strength owing to the welding. The UTS of PCGTAW joints is 1167 MPa, lower by 3% compared with the BM; however, it is higher by approximately 3% than that of the unpulsed joints. It can be seen from Fig. 6, the unpulsed and pulsed welds exhibit much lower ductility, particularly in the GTAW joints. The poor ductility of weldments is attributed to

the presence of α' martensites [12] and the addition of TiB reinforcements [9] in the fusion zone. The elongation of base metal is 8.14%. While, the elongation of unpulsed joints is 4% and that of pulsed joints is 5.1%. This shows that there are 51% and 39% reduction in ductility due to the effect of welding thermal cycle. However, the PCGTAW joints display higher ductility, which is increased by 28% than the unpulsed joints, due to the refinement microstructure and network structure of TiB in the weld. It should be pointed out that the failures in the welded tensile samples are mostly located in the base metal region, which shows that the real weld strength is higher than the obtained results.

With increasing temperature, the UTS decreases but the elongation increases. At 873 K, the UTS of unpulsed joints is 706 MPa, almost up to 96% of the BM strength (737 MPa). Significantly, the UTS of pulsed joint is 763 MPa superior to the BM strength, which is increased by 8% compared with the unpulsed joint. At 923 K, the UTS of pulsed joint is 615 MPa, increased by 5% compared with the unpulsed weld (585 MPa), and both higher than the BM strength (550 MPa). The overmatching weld joint is obtained. This proves that the pulsed joint displays the lowest reduction rate in strength than the unpulsed joint and base metal with increasing temperature. However, both the unpulsed and pulsed joints exhibit good ductility compared with the BM and increase with increasing temperature [2]. The elongation of pulsed joint is 7% higher than that of the unpulsed joint at 873 K because of the refinement microstructure and network structure of TiB in the weld. As the test temperature is 923 K, the difference in elongation between the welded joint and base metal becomes closer, and this is mainly ascribed to the greater softening effect of the matrix alloy [20].

In the as-welded condition, especially at high temperatures the joint prepared by PCGATW shows higher UTS and ductility compared with that without current pulsing. Due to the greater cooling rate of current pulsing, there are many α' martensites and the saturation ratio of α' in pulsed condition is higher than that in unpulsed condition. Moreover, the grain refinement in β columnar grain sizes due to pulsing is believed to be responsible for the improvement in strength and ductility, and thus the joint strength is improved. The similar results were found in the previous research work [15]. On the other hand, TiB_w reinforcements in the weld also strengthen the butt joint through the load transfer effect by the shear-lag mechanism [3]. The network-boundary strengthening mechanism is regarded as an effective factor in improving the elevated temperature mechanical properties [20], and the network boundary containing TiB_w (Figs. 3 and 4) still plays a significant strengthening effect on the butt joint even at higher temperatures, which agrees with the published research [5].

4 Conclusions

The effect of pulsing current on gas tungsten arc welded discontinuously reinforced titanium matrix composites was investigated. Current pulsing in GTAW has lead to relatively finer grain structure in TMCs welds. The grain refinement, much smaller size and network structure of TiB whiskers in the weld due to current pulsing result in increase in the hardness, strength and ductility of the PCGAT welded joints. The butt joints fabricated by PCGTAW show higher tensile strength whether at room or elevated temperature, and the pulsed weld exhibits a much slower reduction rate in strength and reaches the full-strength, even higher than the base metal strength. The enhancement in strength of pulsed joint is approximately by 3% and 8% at room and elevated temperature respectively compared with the unpulsed joints. The average hardness of pulsed joints in the fusion zone reaches the peak value of 548 $HV_{0.2}$, which is higher by 3% than that of the unpulsed joint. The hardness of pulsed welds shows a lower scatter extent.

References

[1] XIAO L, LU W J, QIN J N, CHEN Y F, ZHANG D, WANG M M, ZHU F, JI B. Creep behaviors and stress regions of hybrid reinforced high temperature titanium matrix composite [J]. Composites Science Technology, 2009, 69: 1925−1931.

[2] LI J X, WANG L Q, QIN J N, CHEN Y F, LU W J, ZHANG D. Thermal stability of in situ synthesized (TiB+La_2O_3)/Ti composite [J]. Materials Science Engineering A, 2011, 528: 4883−4887.

[3] ZHANG Z G, QIN J N, ZHANG Z W, CHEN Y F, LU W J, ZHANG D. Microstructure effect on mechanical properties of in situ synthesized titanium matrix composite reinforced with TiB and La_2O_3 [J]. Materials Letters, 2010, 64: 361−363.

[4] TJONG S C, MAI Y W. Processing-structure-property aspects of particulate- and whisker-reinforced titanium matrix composites [J]. Composites Science Technology, 2008, 68: 583−601.

[5] MAO J W, WANG M M, WANG L Q, XUW X B, LU W J, ZHANG D, QIN J N, SUN X J, ZHU X X. Weld zone characteristic and mechanical performance of in situ titanium matrix composites using gas tungsten arc welding (GTAW) [J]. Science Technology of Welding and Joining, 2012, 17: 630−635.

[6] HIROSE A, MATSUHIRO Y, KOTOH M, KOBAYASHI K F. Laser-beam welding of SiC fibre-reinforced Ti−6Al−4V composite [J]. Journal of Materials Science, 1993, 28: 349−355.

[7] ANTONIO M A D S, JORGE F D S, STROHAECKER T R. An investigation of the fracture behaviour of diffusion-bonded Ti6Al4V/TiC/10p [J]. Composites Science Technology, 2006, 66: 2063−2068.

[8] KUMARA A, SAPP M, VINCELLI J, GUPTAA C. A study on laser cleaning and pulsed gas tungsten arc welding of Ti−3Al−2.5V alloy tubes [J]. Journal of Materials Processing Technology, 2010, 21: 64−71.

[9] BALASUBRAMANIAN V, JAYABALAN V, BALASUBRAMANIAN M. Effect of current pulsing on tensile properties of titanium alloy [J]. Materials Design, 2008, 29: 1459−1466.

[10] YANG M X, QI B J, CONG B Q, LIU F J, YANG Z. Effect of pulse frequency on microstructure and properties of Ti−6Al−4V by ultrahigh-frequency pulse gas tungsten arc welding [J]. International Journal of Advanced Manufacturing Technology, 2013, 68: 19−13.

[11] BALASUBRAMANIAN M, JAYABALAN V, BALASUBRAMANIAN V. Optimizing the pulsed current gas tungsten arc welding parameters [J]. Journal of Materials Science and Technology, 2006, 22: 821−825.

[12] BABU N K, GANESH S S R, MYTHILI R, SAROJA S. Correlation of microstructure with mechanical properties of TIG weldments of Ti−6Al−4V made with and without current pulsing [J]. Materials Characterization, 2007, 58: 581−587.

[13] BALASUBRAMANIAN M, JAYABALAN V, BALASUBRAMANIAN V. Effect of pulsed current gas tungsten arc welding parameters on microstructure of titanium alloy welds [J]. Journal of Manufacturing and Engineering-ASME, 2009, 131: 064501.

[14] XIAO L, LU W J, QIN J N, CHEN Y F, ZHANG D, WANG M M, ZHU F, JI B. Steady state creep of in situ TiB plus La_2O_3 reinforced high temperature titanium matrix composite [J]. Materials Science and Engineering A, 2009, 499: 500−506.

[15] SUNDARESAN S, JANAKI R G D, MADHUSUDHAN R G. Microstructural refinement of weld fusion zones in α-β titanium alloy using pulsed current welding [J]. Materials Science and Engineering A, 1999, 262: 88−100.

[16] ATAPOUR M, ZAHRANI E M, SHAMANIAN M, FATHI M H. Corrosion behavior and galvanic corrosion studies of Ti−6Al−4V alloy GTA weldment in HCl solution [C]//TSM Supplemental Proceedings: Materials Fabrication, Properties, Characterization, and Modeling. New Jersey: Wiley, 2011: 707−714.

[17] HIRATA Y. Pulsed arc welding [J]. Welding International, 2003, 17: 98−115.

[18] PADMANABAN G, BALASUBRAMANIAN V. Metallurgical characterization of pulsed current gas tungsten arc, friction stir and laser beam welded AZ31B magnesium alloy joints [J]. Materials Chemistry and Physics, 2011, 125: 686−697.

[19] ANTONIO M A D S, AXEL M, JORGE F D S, CARLOS E F K, TELMO R S. Mechanical and metallurgical properties of friction-welded TiC particulate reinforced Ti−6Al−4V [J]. Composites Science Technology, 2004, 64: 1495−1501.

[20] HUANG L J, GENG L, PENG H X, KAVEENDRAN B. High temperature tensile properties of in situ TiB_w/Ti6Al4V composites with a novel network reinforcement architecture [J]. Materials Science and Engineering A, 2012, 534: 688−692.

有、无脉冲电流制备的钛基复合材料钨极氩弧焊接件的组织与力学性能

毛建伟，吕维洁，王立强，张 荻，覃继宁

上海交通大学 金属基复合材料国家重点实验室，上海 200240

摘 要：研究脉冲电流对不同温度下的钛基复合材料钨极氩弧焊接头的显微组织、硬度和拉伸性能的影响。采用或不采用脉冲电流，均能得到全熔透的对接焊接头。运用光学显微技术、硬度测试和扫描电镜观察对焊接接头的冶金特性进行分析，研究不同温度下与显微组织密切相关的焊接接头的拉伸性能。结果表明，脉冲电流导致焊缝区的显微组织和 TiB 晶须尺寸显著细化，并改变 TiB 增强体的重新分布状态，从而使得脉冲焊接接头具有较高的硬度、拉伸强度和伸长率。

关键词：钛基复合材料；脉冲电流；焊接；力学性能；晶粒细化；显微组织

(Edited by Xiang-qun LI)